Spatial mode cleaning by femtosecond filamentation in air

B. Prade, M. Franco, and A. Mysyrowicz

Laboratoire d'Optique Appliquée, Ecole Nationale Supérieure de Techniques Avancées, Ecole Polytechnique, CNRS UMR 7639, Palaiseau F-91761, France

A. Couairon

Centre de Physique Théorique, École Polytechnique, CNRS UMR 7644, Palaiseau F-91128, France

H. Buersing, B. Eberle, M. Krenz, and D. Seiffer

FGAN-Forschungsinstitut für Optronik und Mustererkennung, Research Institute for Optronics and Pattern Recognition, D-76275 Ettlingen, Germany

O. Vasseur

Office National d'Etudes de Recherches Aérospatiales, Département d'Optique Théorique et Appliquée, Palaiseau, F-91761 France

Received April 12, 2006; revised May 29, 2006; accepted May 31, 2006;
posted June 14, 2006 (Doc. ID 69906); published August 9, 2006

By studying the conical emission of a blue femtosecond laser filament in air, it is shown that self-improvement of the beams' spatial mode quality occurs for a self-guided laser pulse. © 2006 Optical Society of America

OCIS codes: 190.5940, 190.7110, 010.1300.

A significant reshaping of the characteristics of intense femtosecond laser pulses takes place during their nonlinear propagation in air and other gases.[1] The beam first shrinks because of self-focusing and then maintains an $\sim 100\ \mu$m diameter and a peak intensity close to $10^{13}\ \mathrm{W/cm^2}$ over a distance longer than the Rayleigh length. This self-guiding reflects a competition between self-focusing and the defocusing action due to the abrupt onset of multiphoton ionization of air molecules. Optical pulses undergoing filamentation carry other interesting self-actions in terms of spectrum and pulse duration. For instance, the pulse experiences self-compression down to nearly the single-cycle limit.[2–4] Remarkably, the emerging pulse conserves the phase relation between the carrier wave and the pulse envelope, making it a very attractive source for generating even shorter laser pulses in the attosecond range.[2] The spectrum of the pulse displays an important broadening due largely to self-phase modulation induced by the self-steepened back edge of the pulse. Part of this broadband emission is in the form of a characteristic colored conical emission (CE) surrounding the filament core, with bluer frequencies on the outside rings.[5] By analyzing the self-guided pulse in the far field, we demonstrate another interesting effect occurring in air during filamentation, namely, a significant improvement of the beam quality of the emerging pulse, which takes the form of a single transverse mode.

The incident pulse was obtained by frequency doubling the output of a CPA Ti:sapphire laser. The incident laser pulse power at 406 nm (duration, 40 fs; pulse energy, 1 mJ; beam waist, 1.5 mm) was focused with a converging mirror of focal length $f=5.66$ m. Typical shot-to-shot intensity variations were of the order of ±5%. To characterize the beam convergence, the strongly attenuated laser pulse intensity profile was first carefully measured at two locations before the geometric focus. From these data, the geometric focus of the low-intensity beam was determined from linear diffraction theory to be 5.66 m after the focusing mirror. At high intensity ($I_0 \sim 1\ \mathrm{GW/cm^2}$), slightly above the onset of filamentation, the laser pulse diameter shrinks to a diameter of $\sim 100\ \mu$m 3 m before the geometric focus and then maintains this small diameter over 2 m. A total loss by 20% of the beam energy occurs during this propagation stage.

We have examined the far-field pattern of the emerging beam at a distance of 20 m after beam collapse. The emerging beam takes the form of an intense core surrounded by weaker radiation forming the CE. A striking feature is the excellent quality of the CE. This is shown in Fig. 1, which compares the spatial profile of the CE [Fig. 1(a)] with the total beam profile at the same distance [Fig. 1(b)]. The total beam comprises the nonfilamentary part of the

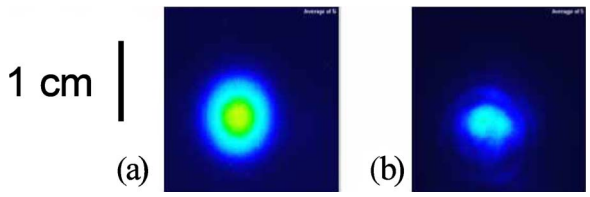

Fig. 1. (Color online) CE and laser pattern measured after 20 m of propagation in air. (a) Surrounding CE only, with the power spectrum close to that of the incident laser pulse removed by a color filter placed at $z=10$ m. The wavelengths between 380 and 420 nm have been removed. (b) Total laser beam (strongly attenuated) at the same distance (false colors).

0146-9592/06/172601-3/$15.00

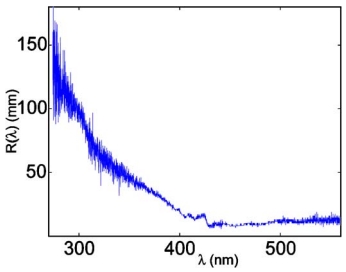

Fig. 2. (Color online) Radius of the CE (half-width at half-maximum) as a function of wavelength measured at 15 m.

beam, the filament core, and the much weaker CE. The conical spatial profile shown in Fig. 1(a) corresponds to a fundamental transverse radiation mode, while the nonfilamentary part of the beam around 400 nm exhibits a poorer beam quality. We have measured the diameter of the CE for different wavelengths with a spectrograph and a CCD camera. Each wavelength has a corresponding quasi-Gaussian profile, the half-width of which is plotted in Fig. 2. Bluer wavelengths exhibit larger diameters, giving rise to the appearance of colored rings, while the CE is absent from the visible part of the spectrum. This allows us to estimate the diameter of the beam around 400 nm that corresponds to the filamentary mode that produces the CE. The fraction of the incoming beam energy that couples into this transverse mode is found to be about 30%. This corresponds to 8 times the critical power estimated from the formula $P_{cr}=3.77\lambda^2/8\pi n_0 n_2$, where λ is the laser wavelength, n_0 is the refractive index, and n_2, is the nonlinear Kerr coefficient at λ.[6] Moll *et al.*[7] reported a similar effect occurring during the collapse of a short pulse propagating in a dense dielectric medium. They found a universal behavior with the beam shape becoming highly radially symmetric when approaching the collapse region. They discussed this effect in terms of the beam's being driven into a Townes mode when the pulse approaches the collapse region. Our results confirm this symmetrization effect in a gas and further show that the high-quality mode is maintained over a large distance exceeding 15 m beyond the collapse location. We compared the measured beam profiles at different distances with those obtained by numerically solving the nonlinear Schrödinger (NLS) equation describing the propagation of an intense pulse in the envelope approximation.[8,9] Interestingly, the experimental results could be reproduced only if an input pulse energy of 0.3 mJ was introduced in the simulations. This corresponds to the fraction of energy coupled in the filamentary mode, as discussed above. All other laser parameters were taken from the experimental conditions. Figure 3(a) shows the calculated peak intensity of the pulse as a function of the propagation distance, together with the free electron density resulting from multiphoton ionization, while Fig. 3(b) shows the evolution of the beam width, computed as contours of the fluence distribution at various levels of the peak fluence. Despite the apparent equilibrium that maintains a constant filament width over 2 m, two distinct bursts of electron density indicate the competition between self-focusing and plasma defocusing taking place in the filament, among other effects.

Figure 4 compares the calculated and the measured fluence profiles at 20 m. It clearly shows the presence of an intense core surrounded by the weaker CE. The fluence profiles between 3 and 5 m were estimated from microburns of undeveloped photographic plates to be of the order of 100 μm, in agreement with the simulations.

Another stringent test of the validity of the simulations concerns the spectral domain. The measured spectrum of the filament core at 20 m, integrated over many shots, is shown in Fig. 5, together with a numerical simulation. There is excellent agreement, except for the lack of fringes in the measured spectrum. However, we observed fluctuations in the fringe pattern from shot to shot. When integrated over several shots, such fluctuations wash out the fringe pattern. We also note that the UV extension (below 300 nm) corresponds to a large angle component in the CE with a radius of the order of 10 cm (see Fig. 2), which is not reproduced in the simulations.

The origin of the fluctuations of the fringe pattern was determined by simulations in which the input intensity was slightly varied around the nominal value. The fringe pattern depends sensitively on the exact intensity. This is illustrated in Fig. 6 by two simulations performed with identical input conditions, except for a change of intensity by 10%. These spectra

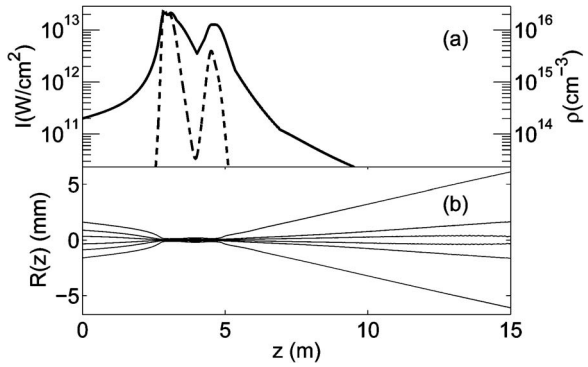

Fig. 3. (a) Calculated peak intensity (solid curve) of the pulse at 406 nm as a function of propagation distance. Also shown is the density of generated free electrons (dashed curve). (b) Calculated beam width as a function of distance. The curves correspond to contours for the fluence distribution at 90%, 50% and 10% of the maximum fluence at each distance.

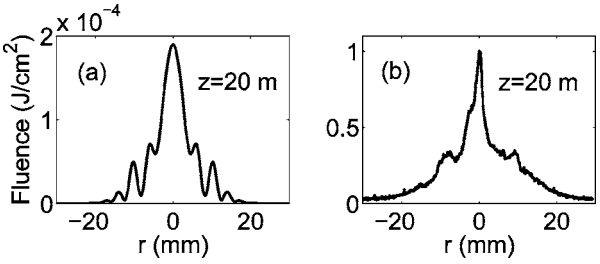

Fig. 4. (a) Calculated and (b) measured beam intensity profile at 20 m, showing the presence of a narrow core surrounded by a weaker ring.

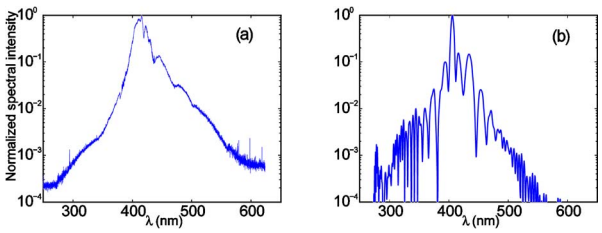

Fig. 5. (Color online) (a) Spectrum of the filament measured on axis after 15 m of propagation. The recorded spectrum is averaged over 100 laser shots (collecting angle, 0.16 mrad). (b) Numerical simulation obtained with an incident laser energy of 0.4 mJ.

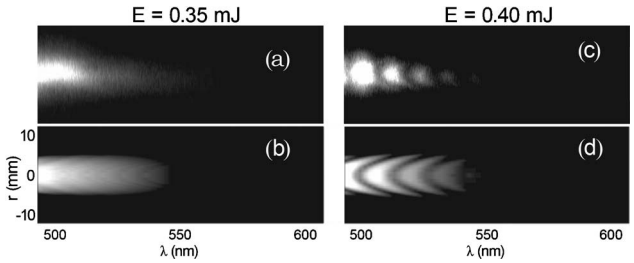

Fig. 6. Comparison between (a), (c) measured and (b), (d) calculated $r-\lambda$ diagram at 10 m for two incident pulse energies. The grayscale is logarithmic with a 2 decade dynamic range.

reproduce rather faithfully the measured single-shot spectra, including the radial expansion of the spectrum with the fishbone structure, as shown in Fig. 6. A similar fishbone structure was obtained from laser pulses undergoing filamentation in various condensed media[10] and was interpreted as a manifestation of the pulse splitting in time that occurs during the filamentation process. Note that close to the filamentation threshold a more uniform spectrum with fewer fringes is observed.

The universality of the filamentation phenomenon, as well as the mode cleaning effect reported in this work, suggests that filaments correspond to attractors of the dynamics of the NLS equation that involve cylindrically symmetric eigensolutions. Recently, several authors proposed that X-waves play a key role in filamentation in water.[10–14] Nonlinear X-waves are nondiffracting and nondispersive spatially and temporally extended solutions to the NLS equation with a characteristic X-shaped extension both in the spectral domain $k_\perp$ versus ω and in the space–time domain (r versus t).[15] Nonlinear X-waves are particularly robust because the losses occurring inside the core are replenished by energy drawn from the extended tails.[11] These structures are spontaneously generated by filaments in condensed media[13] and have led to an interpretation of the associated phenomenon of CE in terms of a four-wave mixing process that involves two highly localized pump waves and two X-waves.[16] The wavelength-dependent angle of the CE measured in different condensed media or in air was shown to be fully determined by the dispersion of the medium.[17] Several simulation results show that far fields exhibit characteristic X-shaped extensions of the laser energy in the region beyond the nonlinear focus[12,14,18] that support the interpretation that mode self-cleaning in air is associated with the generation of a nonlinear X-wave.

In summary, this study reveals a striking new feature associated with filamentation, namely, improved beam quality. Filaments therefore bear remarkable properties in the time (pulse self-compression), frequency (spectrum broadening), and spatial (mode improvement) domains, making them a unique light source for applications.

A. Couairon's e-mail address is couairon@cpht.polytechnique.fr

References

1. A. Couairon, A. Mysyrowicz, K. Yamanouchi, S. L. Chin, P. Agostini, and G. Ferrante, in *Progress in Ultrafast Intense Laser Science* (Springer, 2006), pp. 235–258.
2. C. P. Hauri, W. Kornelis, F. W. Helbing, A. Heinrich, A. Couairon, A. Mysyrowicz, J. Biegert, and U. Keller, Appl. Phys. B: Photophys. Laser Chem. **79**, 673 (2004).
3. A. Couairon, M. Franco, A. Mysyrowicz, J. Biegert, and U. Keller, Opt. Lett. **30**, 2657 (2005).
4. A. Couairon, J. Biegert, C. P. Hauri, W. Kornelis, F. W. Helbing, U. Keller, and A. Mysyrowicz, J. Mod. Opt. **53**, 75 (2005).
5. E. T. J. Nibbering, P. F. Curley, G. Grillon, B. S. Prade, M. A. Franco, F. Salin, and A. Mysyrowicz, Opt. Lett. **21**, 62 (1996).
6. J. H. Marburger, Prog. Quantum Electron. **4**, 35 (1975).
7. K. D. Moll, A. L. Gaeta, and G. Fibich, Phys. Rev. Lett. **90**, 203902 (2003).
8. T. Brabec and F. Krausz, Phys. Rev. Lett. **78**, 3282 (1997).
9. G. Méchain, A. Couairon, M. Franco, B. Prade, and A. Mysyrowicz, Phys. Rev. Lett. **93**, 035003 (2004).
10. D. Faccio, P. Di Trapani, S. Minardi, A. Bramati, F. Bragheri, C. Liberale, V. Degiorgio, A. Dubietis, and A. Matijosius, J. Opt. Soc. Am. B **22**, 862 (2005).
11. A. Dubietis, E. Gaižauskas, G. Tamošauskas, and P. Di Trapani, Phys. Rev. Lett. **92**, 253903 (2004).
12. M. Kolesik, E. M. Wright, and J. V. Moloney, Phys. Rev. Lett. **92**, 253901 1 (2004).
13. D. Faccio, A. Matijosius, A. Dubietis, R. Piskarskas, A. Varanavičius, E. Gaižauskas, A. Piskarskas, A. Couairon, and P. Di Trapani, Phys. Rev. E **72**, 037601 (2005).
14. A. Couairon, E. Gaizauskas, D. Faccio, A. Dubietis, and P. Di Trapani, Phys. Rev. E **73**, 016608 (2006).
15. C. Conti, S. Trillo, P. Di Trapani, G. Valiulis, A. Piskarskas, O. Jedrkiewicz, and J. Trull, Phys. Rev. Lett. **90**, 170406 (2003).
16. D. Faccio, M. Porras, A. Dubietis, F. Bragheri, A. Couairon, and P. Di Trapani, Phys. Rev. Lett. **96**, 193901 (2006).
17. D. Faccio, M. A. Porras, A. Dubietis, A. Tamošauskas, E. Kučinskas, A. Couairon, and P. Di Trapani, Opt. Commun. (2006), doi:10.1016/j.optcom.2006.04.062.
18. M. Kolesik, E. M. Wright, and J. V. Moloney, Opt. Express **13**, 10729 (2005).